

Lotus Seed Green Embryo Extract and a Purified Glycosyloxyflavone Constituent, Narcissoside, Activate TRPV1 Channels in Dorsal Root Ganglion Sensory Neurons

Taewoong Ha,^{||} Mi-Sun Kim,^{||} Bokeum Kang, Kyungmin Kim, Seong Su Hong, Taek Kang, Junhyuk Woo, Kyungreem Han, Uhtaek Oh, Chun Whan Choi,^{*} and Gyu-Sang Hong^{*}



Cite This: <https://doi.org/10.1021/acs.jafc.1c07724>



Read Online

ACCESS |



Metrics & More



Article Recommendations



Supporting Information

ABSTRACT: Several studies have documented the broad-spectrum bioactivities of a lotus seed (*Plumula nelumbinis* [PN]) green embryo extract. However, the specific bioactive components and associated molecular mechanisms remain largely unknown. This study aimed to identify the ion channel-activating mechanisms of PN extracts. Using fluorometric imaging and patch-clamp recordings, PN extracts were screened for calcium channel activation in dorsal root ganglion (DRG) neurons. The TRPV1 channels in DRG neurons were strongly activated by the PN extract (mean amplitude of 131 ± 45 pA at $200 \mu\text{g/mL}$) and its purified glycosyloxyflavone narcissoside (401 ± 271 pA at $100 \mu\text{M}$). Serial treatment with a $200 \mu\text{g/mL}$ PN extract in TRPV1-overexpressing HEK293T cells induced robust desensitization to $10 \pm 10\%$ of the initial current amplitude. Thus, we propose that the PN extract and narcissoside function as TRPV1 agonists. This new finding may advance our knowledge regarding the traditional and scientific functions of PN in human health and disease.

KEYWORDS: green embryo of lotus seed, narcissoside, TRPV1, ion channel, sensory neuron

INTRODUCTION

The seeds, flowers, leaves, and stamina of the sacred lotus *Nelumbo nucifera* have long been used as medicinal herbs and functional foods in Asia and Africa.¹ The green embryo of the lotus seed (*Plumula nelumbinis* [PN]) is widely consumed as a healthy food in Asia, and its dried form is also used in herbal tea. The consumption of PN improves immune system functions, alleviates high blood pressure, and relieves internal heat or dryness.² These effects are mediated through phytochemicals and flavonoids found in the PN extract, some of which are now recognized for their antioxidant, anti-inflammatory, cardioprotective, and antitumor activities.^{3–5} However, many of the compounds responsible for the bioactivities of the PN extract remain unidentified, and the molecular mechanisms of some compounds are still unknown; this limits physiological studies and further development of healthy foods and pharmaceutical drugs.

Flavonoids are prominent secondary metabolites of plants. Several benefits of flavonoids have been documented in human health and nutrition.⁶ A large number of these phytochemicals have been isolated, and their roles as antioxidants, antibacterial agents, cardioprotectants, anti-inflammatory agents, and immune system regulators have been demonstrated.⁷ Narcissoside (NAR), also known as narcissin, is a glycosyloxyflavone (flavonol glycoside) present in a number of medicinal plant tissues such as the *Gynura divaricate* leaves, *Mondrinda citrifolia* fruits, and *Sophora japonica* flowers (Flos Sophorae Immaturos).^{8–10} Recent studies suggest that NAR has an antioxidant activity and exerts an inhibitory effect on tyrosinase,^{11,12} however, the complete spectrum of its bioactivity is obscure.

Transient receptor potential vanilloid 1 (TRPV1) is a widely studied nonselective cation channel substantially present in sensory neurons and their nerve endings that are directly and indirectly activated by capsaicin (CAP), noxious heat, ethanol, protons (or acid), and various endogenous signaling molecules such as inflammatory mediators.^{13–15} Various compounds present in foods, such as allicin in garlic, piperine in black pepper, and gingerol in ginger, rapidly trigger TRPV1 channel opening.^{16–18} Detection of these cues by subcutaneous TRPV1-positive nerve endings of dorsal root ganglion (DRG) sensory neurons transduces and transmits nociceptive signals to the central nervous system. Therefore, TRPV1 acts as an inflammatory pain and noxious heat sensor. Much effort has been devoted to the identification or development of TRPV1 antagonists useful as clinical analgesics. However, owing to side effects such as increased core body temperature and augmented pain sensitivity observed in clinical trials, no such agents have been approved for clinical use yet.¹⁹ As an alternative, TRPV1 agonists and desensitizers may be potential drug candidates for inflammatory and chronic pain.²⁰

In this study, we assessed if a crude PN extract and its constituent NAR activate TRPV1 in DRG sensory neurons.

Received: December 2, 2021

Revised: March 9, 2022

Accepted: March 15, 2022

Our study identified the PN extract as a potential source of TRPV1-modulating agents for pain treatment.

MATERIALS AND METHODS

Chemicals, Genes, and Transfection Vectors. NAR was purified from a PN extract as described in the following section. Dulbecco's modified Eagle's medium (DMEM) with high glucose, penicillin and streptomycin, and fetal bovine serum (FBS) was purchased from HyClone Laboratories Inc. or ThermoFisher Scientific. Molecular-grade allyl-isothiocyanate (AITC), camphor, GSK1016790A, and the TRPV1 agonist CAP were purchased from Sigma-Aldrich, and lysophosphatidylcholine (LPC) was purchased from Fluka-BioChemka. The cDNAs encoding human *Trpv1* (Gene ID: 7442), *Trpv2* (Gene ID: 51393), *Trpv3* (Gene ID: 162514), *Trpv4* (Gene ID: 59341), and *Trpa1* (Gene ID: 8989) were cloned and inserted into the pCDNA3.1(+) vector for cell transfection and subsequent calcium ion (Ca^{2+}) imaging. For patch-clamp experiments, these genes were cloned into pEGFP-N1 for fluorescent marking. For Ca^{2+} imaging experiments using pEGFP-N1, the vector was mutated to include stop codons between the gene and the GFP sequence (pEGFP-N1[STOP]). All cDNA clones were verified through sequencing.

Isolation and Identification of PN Extract Constituents. Analytical thin-layer chromatography was performed using precoated silica gel 60 F254 (Merck, Germany), silica gel 60 RP-18 F₂₅₄S plates (Merck, Germany), column chromatography with octadecyl-silica (ODS)-A (12 nm S-7 μm , YMC GEL, Japan), and preparative HPLC with an LC-8A pump (Shimadzu, Kyoto, Japan). Both ^1H and ^{13}C NMR spectra were recorded using a Bruker Ascend 700 MHz spectrometer with tetramethylsilane as an internal standard. LC-ESI-MS data were obtained on a Triple TOF 5600+ instrument (AB SCIEX).

HEK297T Cell Culture and Transfection. HEK297T (HEK) cells were obtained from the American Type Culture Collection (Manassas, VA). Cells were maintained in a basal culture medium of DMEM (Gibco, TX) supplemented with 10% heat-inactivated FBS and 1% penicillin–streptomycin (Sigma-Aldrich) on glass coverslips in 35 mm dishes. Cells were transfected with a pIRES2-AcGFP1-TRPV1 vector for 48 h using a FuGene Transfection Reagent (Promega, WI).

Isolation of DRG Neurons. Primary DRG neurons were isolated as previously described.²¹ Briefly, thoracic and lumbar DRGs were dissected from 6-week-old mice and collected in ice-cold DMEM/F12 (Life Technologies, CA), washed thrice with fresh DMEM/F12, and then incubated in a digestion medium containing 2 mg/mL collagenase IA (Sigma-Aldrich) for 45 min at 37 °C. Ganglia were then washed gently twice or thrice in DMEM/F12 supplemented with 10% heat-inactivated FBS, 1% penicillin–streptomycin, 50 ng/mL nerve growth factor (Life Technologies), and 5 ng/mL glial-derived neurotrophic factor (Life Technologies). After two washes in this medium, ganglia were resuspended and gently triturated with a 1 mL pipette prepped in FBS. Separated cells were plated onto round glass coverslips (ThermoFisher Scientific) and maintained in a 95% air/5% CO_2 gas mixture at 37 °C for 48–72 h before experiments.

Current Recordings. TRPV1 currents were measured in both whole-cell and inside-out patch-clamp modes. Whole-cell currents were measured by rupturing the plasma membrane under a 2–3 M Ω glass pipette after giga-seal formation. The junctional potentials were adjusted to 0 and the holding potential was set to –60 mV for whole-cell or +60 mV for inside-out patch clamping.

All currents were amplified and filtered at 0.5 Hz using an Axopatch200B amplifier (Molecular Devices, San Jose, CA), digitized at 5 kHz using a Digidata 1440 digitizer (Molecular Devices), and recorded to computer disk for offline analysis using pClamp version 10.0 (Molecular Devices). The pipette solution for recording whole-cell currents from HEK cells and DRG neurons contained 130 mM CsCl, 2 mM MgCl_2 , 10 mM HEPES, 2 mM Mg-ATP, 0.2 mM Na-GTP, and 25 mM D-mannitol. The pH was set to 7.2 with CsOH, and the osmolarity was adjusted to 300 mOsm/kg by adding D-mannitol.

The bath solution contained 130 mM NaCl, 5 mM KCl, 2 mM CaCl_2 , 2 mM MgCl_2 , and 10 mM HEPES. The osmolarity was adjusted to 306 mOsm/kg by adding 10 mM D-mannitol, and the pH was set to 7.2 by adding NaOH. For inside-out patch-clamp recording, the pipette and bath solutions were switched. In activator experiments, a 100 $\mu\text{g}/\text{mL}$ PN extract and 1 μM CAP (Sigma-Aldrich) were added to the bath solution.

Ca^{2+} Imaging. Intracellular Ca^{2+} was measured as previously described.²² Briefly, HEK cells transfected with *Trpv1*, *Trpv2*, *Trpv3*, *Trpv4*, or *Trpa1* and primary DRG neurons were incubated for 30 min with 2 μM Fluo-3/AM (Life Technologies) and 0.02% (wt/vol) Pluronic F-127 (Sigma-Aldrich) in buffer containing 140 mM NaCl, 2 mM MgCl_2 , 5 mM KCl, 10 mM HEPES, and 2 mM CaCl_2 with the pH adjusted to 7.2 using NaOH and the osmolarity adjusted to 306 mOsm/kg with D-mannitol. Imaging was performed at room temperature (23–25 °C) using a confocal microscope (Carl Zeiss, LSM 800) equipped with an Alexa Fluor 488 nm filter. Ca^{2+} -sensitive Fluo-3 fluorescence was recorded for 200 s at a rate of 1 frame every 2 s. For each trial, ~100 images (512 \times 512 pixels resolution) were acquired at 0.5 \times digital zoom using a 20 \times objective. A drug-containing solution was added to the recording chamber using a pressurized micropipette after 20–30 s (10–15 frames) of baseline recording. For inhibition experiments, Ca^{2+} signals were recorded from HEK cells expressing TRPV1 for 20 s before the application of CAP (1 μM). After 120 s of Fluo-3 fluorescence recording, capsaizepine (CPZ, 10 μM) (MedChemExpress, NJ), vehicle, or PN extract was administered, and the reduction in fluorescence emission was then measured. Cells were treated with 1 μM thapsigargin (Sigma-Aldrich), a noncompetitive sarcoplasmic reticulum (SR)/endoplasmic reticulum (ER) Ca^{2+} ATPase (SERCA) inhibitor, for 400 s before the measurement of the Ca^{2+} influx. Sample fluorescence images and images used for quantitative analysis were obtained at the peak fluorescence brightness (correlated with peak intracellular free Ca^{2+} in the absence of photobleaching). Fluorescence intensity was measured using ImageJ (NIH, Bethesda, MD).

Molecular Docking. The simulations were performed on one of four subunits of the protein using the AutoDock Vina program (version 1.2.3)^{23,24} with the Amber force field.^{25,26} Missing atoms were added, and the hydrogen-bond network was optimized using PDB2PQR 2.1.²⁷ The protonation states of the model were titrated using PROPKA 3.1.²⁸ The searching for the binding sites of NAR was conducted on the search spaces defined by 125 cubic boxes of 30 Å edge covering the whole protein. The randomly chosen 32 binding conformations were used for each cubic box. The AutoDock Vina program is based on a local search global optimizer: each step of the optimization involves a random perturbation of the conformation followed by an evaluation of the scoring function as well as its derivatives in the position–orientation–torsion coordinates. The Broyden–Fletcher–Goldfarb–Shanno (BFGS) method was used for the local optimization procedure using both the scoring function and its gradient.²⁹ The scoring function is based on the Amber force field that includes van der Waals, electrostatic, directional hydrogen-bond potentials, a pairwise additive desolvation term based on partial charges, and a simple conformational entropy penalty.^{25,26} The number of evaluations in a local optimization is determined heuristically, depending on the size and flexibility of the ligand and the flexible side chains, guided by convergence and other criteria.^{23,24}

Statistical Analysis. All statistical analyses were performed using SigmaPlot (SYSTAT, San Jose, CA) and presented as the mean \pm standard error of the mean from at least three independent experiments. Group means were compared using Student's *t*-test or one-way analysis of variance (ANOVA) with Dunn's post hoc test unless otherwise indicated. **p*-values < 0.05, ***p*-values < 0.01, and ****p*-values < 0.001 were considered significant.

RESULTS

PN Extract Activates Ca^{2+} -Permeable Channels in DRG Sensory Neurons. Peripheral sensory neurons express several ion channels, including multiple Ca^{2+} -permeable

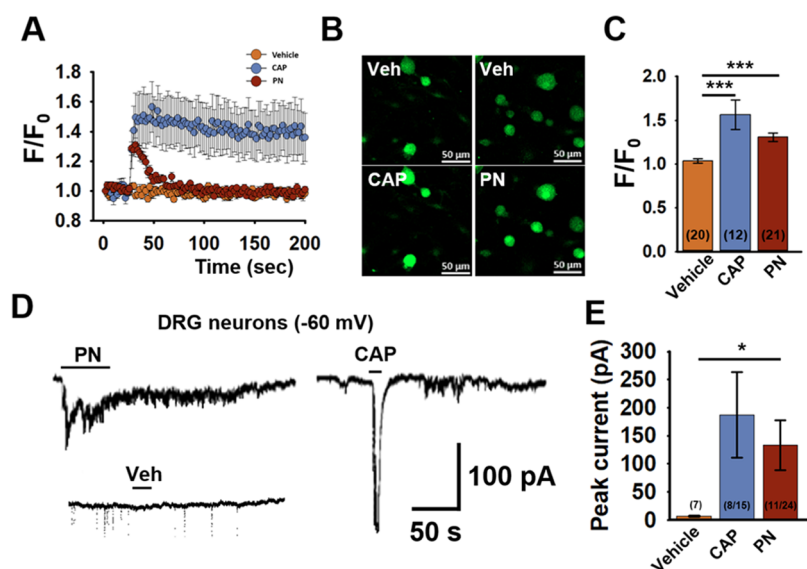


Figure 1. Activation of TRPV1 channel-mediated Ca²⁺ signals and membrane currents by the PN extract in dorsal root ganglion (DRG) sensory neurons. (A) Increases in the intracellular Ca²⁺ concentration induced by bath application of the specific TRPV1 agonist CAP (1 μM) or PN extract (PN) (100 μg/mL). *F* indicates the fluorescence emission intensity of the Ca²⁺-sensitive dye Fluo-3/AM, and *F*₀ indicates the initial fluorescence intensity. (B) Representative confocal images of Fluo-3-loaded DRG neurons after application of vehicle and then either CAP or PN extract. An increase in fluorescence emission (green) indicates an increased intracellular Ca²⁺ concentration. (C) Summary of mean peak Ca²⁺ (peak *F*/*F*₀) in DRG neurons treated with the vehicle, CAP, or PN extract. The numbers in the bracket indicate the number of cells tested in all bar graphs. ****p* < 0.001 for one-way analysis of variance (ANOVA) with post hoc Dunn's tests for pairwise comparisons. (D) Representative cationic currents recorded in DRG neurons during the bath application of the 200 μg/mL PN extract, the vehicle, or 1 μM CAP. (E) Average peak currents evoked by vehicle, CAP, and PN extract. Data were obtained from the responding neurons; CAP: 8 of 15 neurons and PN: 11 of 24 neurons. **p* < 0.05 for one-way ANOVA with post hoc Dunn's tests.

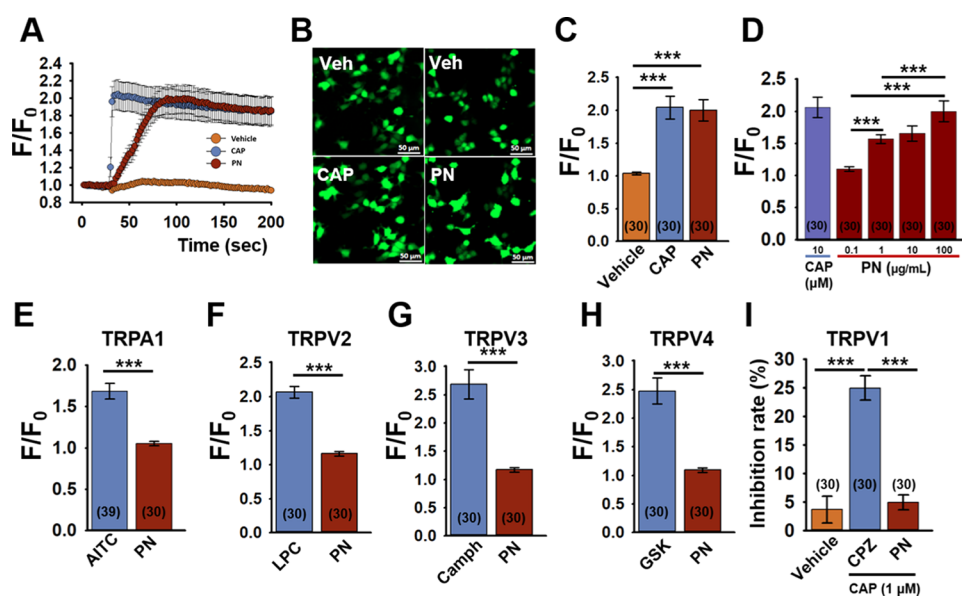


Figure 2. Induction of Ca²⁺ signals by the PN extract, specifically in TRPV1-overexpressing HEK cells. (A) Increases in the intracellular Ca²⁺ concentration induced by the application of CAP (10 μM) or the PN extract (100 μg/mL) as indicated by Fluo-3 fluorescence emission. (B) Representative confocal images of TRPV1-overexpressing Fluo-3-HEK cells after application of the vehicle, followed by CAP (10 μM) or the PN extract (100 μg/mL) application. Greater fluorescence emission indicates a high concentration of intracellular Ca²⁺. (C) Mean peak Ca²⁺ (peak *F*/*F*₀). (D) Dependence of the peak Ca²⁺ elevation (*F*/*F*₀) on the PN extract concentration. (E–H) Average peak Ca²⁺ responses to the PN extract (100 μg/mL) and specific TRP channel agonists in HEK cells overexpressing TRPA1, TRPV2, TRPV3, or TRPV4 (100 μM AITC for TRPA1, 1 μM LPC for TRPV2, 20 mM camphor for TRPV3, and 100 nM GSK1016790A for TRPV4). (I) Comparison of the TRPV1 inhibition rate (% *F*/*F*₀). After TRPV1-dependent Ca²⁺ elevation by 1 μM CAP, vehicle, 10 μM CPZ, and PN extract (100 μg/mL) were applied.

channels, to transduce and transmit external signals. To investigate the effect of a PN ethanol extract on Ca²⁺ channel activity in sensory neurons, we measured intracellular changes in the Ca²⁺ concentration in primary mouse DRG neurons

loaded with the fluorescent Ca²⁺ dye Fluo-3/AM using confocal microscopy. To exclude intracellular increases owing to ion release from the ER, all recordings were performed in the presence of 1 μM thapsigargin, an SR/ER Ca²⁺ ATPase

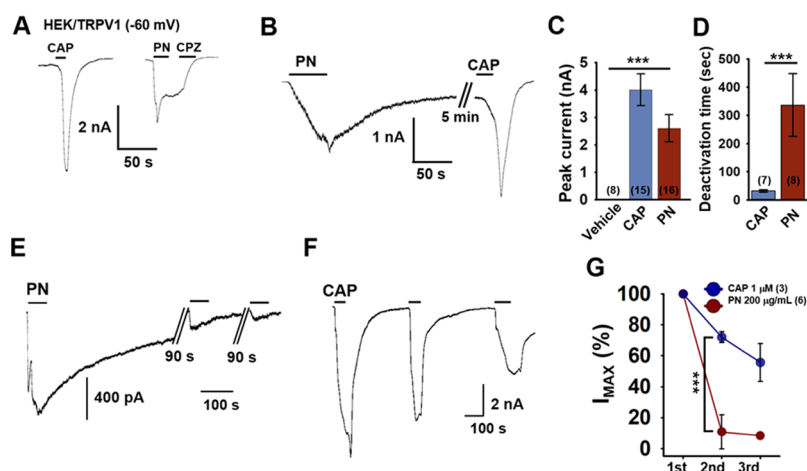


Figure 3. Currents induced by the PN extract exhibited greater desensitization than those induced by CAP. (A) Representative cationic currents induced by CAP (1 μ M) or the PN extract (200 μ g/mL), followed by CPZ (10 μ M), in HEK cells transfected with *Trpv1*. (B) Sequential activation of currents induced by the PN extract and then CAP in one TRPV1-overexpressing HEK cell. (C) Mean peak currents induced by the vehicle, CAP (1 μ M), and PN extract (200 μ g/mL). *** p < 0.001 for one-way analysis of variance (ANOVA) with post hoc Dunn's tests. (D) Mean deactivation time of currents induced by CAP (1 μ M) and the PN extract (200 μ g/mL). *** p < 0.001 for one-way ANOVA with post hoc Dunn's tests. (E, F) Representative traces of currents induced by three consecutive applications of the PN extract (200 μ g/mL) (E) or CAP (1 μ M) (F) in HEK cells transfected with *Trpv1*. (G) Summary of the mean maximal current ratio. Note that that second application of the PN extract induced a current markedly smaller than that noted after the initial application *** p < 0.001 for one-way ANOVA with post hoc Dunn's tests.

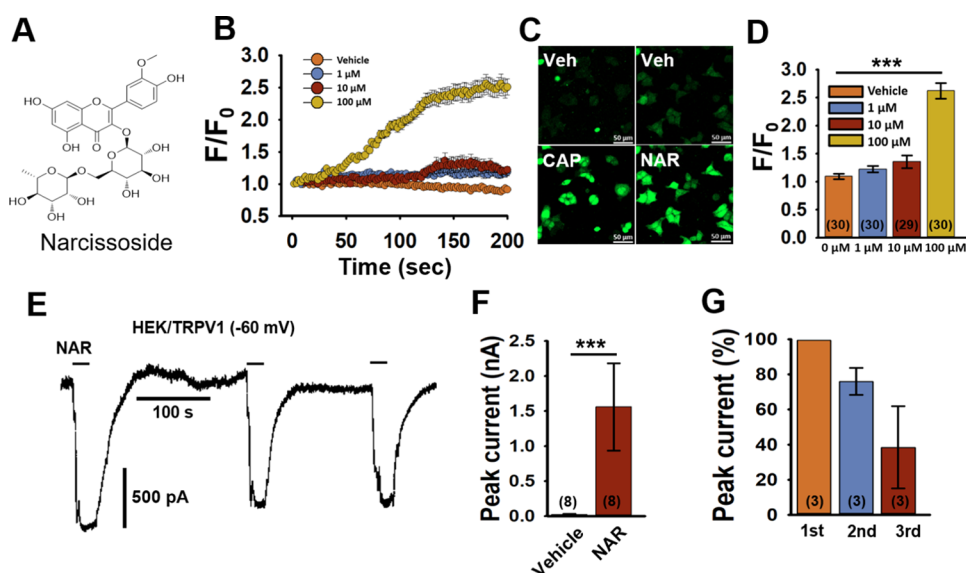


Figure 4. Narcissoside (NAR) purified from the PN extract-activated TRPV1 channels in HEK cells. (A) Molecular structure of NAR. (B) Increases in the intracellular Ca^{2+} concentration induced by vehicle, 1, 10, and 100 μ M NAR. (C) Representative confocal images of Fluo-3-loaded HEK cells overexpressing TRPV1 after the application of vehicle and then CAP (1 μ M) or NAR (100 μ M). (D) Mean peak of Ca^{2+} elevations (F/F_0). (E) Representative cationic currents recorded from *Trpv1*-transfected HEK cells in response to NAR (100 μ M). (F) Average peak currents induced by the vehicle and NAR. (G) Average peak currents induced by three consecutive applications of NAR (100 μ M) showing that these currents are desensitized but not as much as PN extract-induced currents.

inhibitor that blocks Ca^{2+} release from intracellular stores. The application of a 100 μ g/mL PN extract led to a marked increase in Fluo-3 fluorescence emission, indicating an increased intracellular Ca^{2+} concentration (Figure 1A,B); however, the vehicle (DMSO 0.05%) had no effect. The TRPV1 channel against CAP also induced a strong Ca^{2+} signal (Figure 1A,B). However, this increase was markedly longer and also slightly greater in amplitude than that induced by the PN extract (Figure 1C). To further verify that these treatments activate Ca^{2+} -permeable ion channels, currents were measured from DRG neurons via whole-cell patch clamping using an NaCl-based extracellular solution with a 2 mM Ca^{2+} and CsCl-

based intracellular solution to block potassium currents. We targeted relatively small DRG neurons (diameter <25 μ m) for recording, as such cells are more likely TRPV1-positive nociceptive neurons. In this subpopulation, gravity application of a 200 μ g/mL PN extract or 1 μ M CAP to the bath generated inward cation currents at a holding potential of -60 mV, whereas the vehicle showed no effect (Figure 1D). The mean peak current induced by the PN extract (8/15 neurons, 131 ± 45 pA) was similar in amplitude to that induced by CAP (11/24 neurons, 188 ± 75 pA) (Figure 1E).

PN Extract Activates TRPV1 Channels in HEK Cells. We examined if the Ca^{2+} -permeable channels activated by a

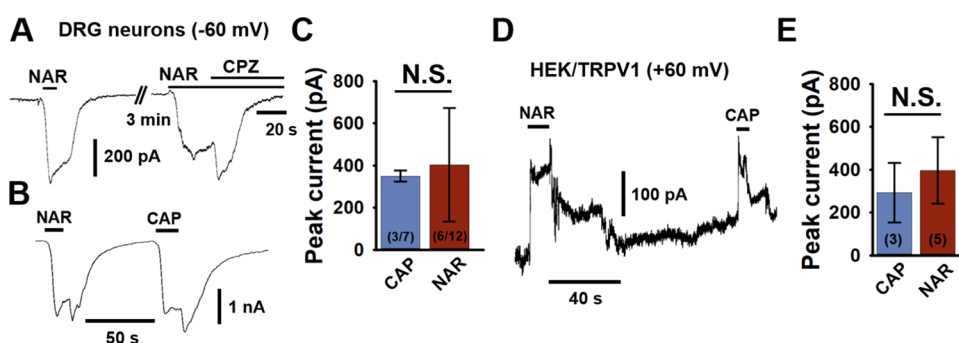


Figure 5. TRPV1-expressing HEK cells are intracellularly activated by NAR, suggesting that NAR-activated current in DRG neurons is mediated by TRPV1. Representative cationic current from a DRG neuron is elicited by two consecutive applications of 100 μM NAR at a 3 min delay. The second NAR-induced current was blocked by 10 μM CPZ. (A, B) Representative trace showing an NAR-induced current, followed by a CAP-induced current, in one DRG neuron. (C) Average peak currents induced by CAP and NAR in DRG neurons. (D) Representative currents at +60 mV holding potential from the inside-out patches of *Trpv1*-transfected HEK cells induced by NAR (100 μM) and CAP (1 μM). (E) Average peak currents from the inside-out patches of HEK cells induced by CAP (1 μM) and NAR (100 μM).

PN extract are of the TRPV family by measuring Ca^{2+} signals in HEK cells transfected with one of *Trpv1*–4 or *Trpa1*. Cells overexpressing TRPV1 demonstrated a robust increase in the Ca^{2+} concentration in response to the PN extract (Figure 2A,B), and the mean peak increase induced by a 100 $\mu\text{g}/\text{mL}$ PN extract was similar to that induced by 10 μM CAP (Figure 2C). Dose–response trials showed that a 0.1 $\mu\text{g}/\text{mL}$ PN extract induced no increase in the Ca^{2+} concentration, whereas a 1, 10, and 100 $\mu\text{g}/\text{mL}$ PN extract induced a robust increase in the Ca^{2+} concentration in TRPV1-overexpressing HEK cells (Figure 2D). In contrast, cells transfected with *Trpa1*, *Trpv2*, *Trpv3*, or *Trpv4* showed no measurable increase in the Ca^{2+} concentration in response to the PN extract but did respond, respectively, to the specific TRPA1 activator AITC (100 μM), TRPV2 activator LPC (1 μM), TRPV3 activator camphor (20 mM), and TRPV4 activator GSK1016790A (100 nM) (Figure 2E–H), confirming that most of the Ca^{2+} influx generating an increase in the Ca^{2+} concentration was mediated through the opening of the TRPV1 channel. We further assessed the potential inhibitory activity of the PN extract on the activation of TRPV1 using 1 μM CAP. The TRPV1-specific antagonist 10 μM CPZ significantly reduced the Ca^{2+} signals, whereas the PN extract did not exhibit any inhibitory activity (Figure 2I).

To further confirm that the Ca^{2+} signal activated by the PN extract is due to TRPV1 channel opening, whole-cell patch-clamp recordings were acquired from *Trpv1*-transfected HEK cells. The application of 1 μM CAP induced an inward current of a mean amplitude 4287 ± 560 pA ($n = 15$), whereas a PN extract elicited a mean current of 2610 ± 495 pA ($n = 16$) at -60 mV (Figure 3A). This large current induced by the PN extract was completely inhibited by 10 μM CPZ; hence, it was mediated entirely by TRPV1. Moreover, CAP still induced a large current 5 min after a PN extract-induced current in the same TRPV1-overexpressing HEK cells (Figure 3B).

Although the PN extract did not inhibit CAP-induced currents, serial applications showed that PN extract-induced TRPV1 currents exhibited a much slower deactivation time than CAP-induced currents (Figure 3D). Furthermore, PN extract-induced currents also demonstrated much greater desensitization. For instance, the second application of CAP induced a current that was still $72 \pm 3\%$ of the initial current amplitude (Figure 3F,G), whereas the second dose of the PN extract induced a TRPV1 current with an amplitude of only $10 \pm 10\%$ of the initial amplitude (Figure 3E,G).

Isolation, Identification, and Functional Characterization of PN Extract Constituents.

We purified potential bioactive phytochemicals from a PN extract and identified one constituent, NAR, which acted as a TRPV1 agonist (Figure 4A). Isolation procedures and the structural data of NAR are shown in Figures S1 and S2. For purification, PN was extracted with 70% ethanol in water. The crude extract was concentrated under reduced pressure, and the ethanol fraction was separated from the aqueous fraction by mixing with *n*-hexane, CH_2Cl_2 , EtOAc, and *n*-BuOH. The EtOAc fraction was then separated through column chromatography using ODS gel and eluted with 10% MeOH in H_2O , yielding eight EtOAc subfractions (EAs 1–8). Fraction EA 6 was purified through preparative HPLC on RP-18 gel and eluted using a step gradient (20–60%) of acetonitrile in H_2O with 0.05% trifluoroacetic acid. The structure of the isolated compound was elucidated using NMR, MS, and UV on the basis of comparisons with reported NAR spectra (Figures S2 and 4A).^{10,30} Final purity was nearly 96%, and the total yield was 12 mg from 91.6 g of the PN extract (Figure S2). However, a previous study has reported a more efficient process that yielded 64.74 mg/100 g NAR from dried PN.³¹

NAR Activates TRPV1 Channels in Transfected HEK Cells. Ca^{2+} imaging experiments and current recordings like those conducted using a PN extract were repeated using purified NAR (Figure 4A). The vehicle (0.05% DMSO), 1 μM CAP, or 100 μM NAR did not induce Ca^{2+} signals in naive HEK cells (Figure S3). However, 1 and 10 μM NAR solutions induced modest increases, and 100 μM NAR induced a robust increase in the Ca^{2+} concentration in TRPV1-overexpressing HEK cells (Figure 4B–D), which was comparable with that induced by CAP. The intensity of Ca^{2+} fluorescence induced by 100 μM NAR revealed robust changes, which were comparable with those induced by 1 μM CAP treatment at the peak point (Figure 4C). Furthermore, 100 μM NAR induced distinct cationic currents (mean = 1.55 ± 0.06 nA, $n = 8$) in TRPV1-overexpressing HEK cells (Figure 4E,F). In contrast to the PN extract treatment, desensitization induced by the second NAR application was indistinguishable from that induced by CAP (Figure 4E,G). Our observations suggest that NAR, a glycosyloxyflavone purified from the PN extract, is a novel TRPV1-specific agonist.

NAR Activates TRPV1 Intracellularly and Induces Cationic Current in TRPV1-Positive Nociceptors. A

subpopulation of DRG neurons was also responsive to 100 μM NAR in addition to 1 μM CAP (Figure 5A), and both compounds, when applied sequentially to the same neuron, induced currents of similar amplitude (3/7 neurons, 401 ± 271 pA by NAR, and 6/12 neurons, 345 ± 22 pA by CAP), suggesting that NAR also activates TRPV1-positive nociceptors (Figure 5B,C). Further analysis was performed with inside-out patches to determine whether NAR also binds to the intracellular side of the open TRPV1 channel. In the inside-out patches at +60 mV, both application of 100 μM NAR and 1 μM CAP activated mean currents of 394 ± 149 and 295 ± 140 pA, respectively (Figure 5D,E), indicating that NAR can activate TRPV1 channels from the intracellular as well as the extracellular side. The effective concentrations of the PN extract and NAR evaluated either through Ca^{2+} imaging or the patch-clamp experiment are shown in Table 1.

Computational Study to Understand the Narcissoside–TRPV1 Interactions. We further characterized the putative binding sites of NAR on TRPV1. The atomic TRPV1 model based on cryoelectron microscope (EM) data was used for docking simulations.³² The 10 most probable binding sites of NAR to TRPV1 were obtained from the docking simulation (Figure 6A). The binding sites are distributed along the subunit, spanning from average binding free energy (E) ranging from -9.15 to -6.50 kcal/mol, except for the cytoplasmic tail part ($z < \sim 20$ Å) (Figure 6B). Binding site 1, which revealed the strongest free energy ($E_1 = -9.15$ kcal/mol) is located in the middle of the subunit ($z = \sim 58$ Å). The amino acid residues that are within 2.2 Å of any atoms in NAR binding site 1 are H410, R500, S502, K504, L506, Y511, S512, K571, and Q700 in the intracellular loop between S4 and S5 regions (Figure 6C). Close-up views of other binding sites (2–10) and putative interacting amino acid residues are also shown in Figure S4. The molecular docking simulation suggests that depending on the conformations of TRPV1, NAR can stably bind to both intracellular and extracellular regions of TRPV1, which is consistent with data from patch-clamp experiments.

DISCUSSION

Many of the traditional claims regarding the health benefits of a PN extract, including the improvement of immune functions, have been verified through both cell- and animal-based research. Various studies have identified functional TRPV1 channels in immune cells. Bujak et al. recently reported that antagonizing TRPV1 in macrophages significantly reduces the release of proinflammatory cytokines.³³ The verification of these molecular mechanisms may facilitate the development of novel anti-inflammatory drugs from PN extracts. Similarly, we demonstrate in this study that the PN extract may suppress TRPV1 activity in nociceptive neurons, suggesting that PN extract constituents can be useful as analgesics.

The primary functions of TRPV1 channels include the regulation of inflammation, pain, and itching.^{13,33,34} TRPV1 channels are substantially present in peripheral nociceptive neurons, including C-fiber nerve endings, and their activation transduces various signals related to inflammation and tissue damage into action potentials that transmit this nociceptive information to the central nervous system. These C-fibers innervate the skin as well as visceral organs such as the lung, stomach, gut, liver, teeth, and gums; therefore, TRPV1 antagonism might have broad clinical applicability in reducing inflammation-associated pain. However, phase-III clinical trials

Table 1. Ca^{2+} Intensity and Electrical Activity after Application of the Effective Concentrations of the PN Extract and NAR in DRG Neurons and TRPV1-Expressing HEK Cells (HEK/TRPV1)

compound	DRG			HEK/TRPV1		
	Ca^{2+} imaging (F/F_0)	patch-clamp whole-cell (pA)	patch-clamp inside-out (pA)	Ca^{2+} imaging (F/F_0)	patch-clamp whole-cell (pA)	patch-clamp inside-out (pA)
vehicle	1	<0	<0	<0	<0	<0
CAP (conc.)	1.6 ± 0.2 (1 μM , $n = 12$)	188 ± 45 (1 μM , $n = 11$)	2.0 ± 0.2 (1 μM , $n = 30$)	4287 ± 560 (1 μM , $n = 15$)	295 ± 140 (1 μM , $n = 3$)	
PN (conc.)	1.3 ± 0.1 (100 $\mu\text{g}/\text{mL}$, $n = 21$)	131 ± 45 (200 $\mu\text{g}/\text{mL}$, $n = 8$)	2.0 ± 0.2 (100 $\mu\text{g}/\text{mL}$, $n = 30$)	2610 ± 495 (200 $\mu\text{g}/\text{mL}$, $n = 16$)		
NAR (conc.)		401 ± 271 (100 μM , $n = 6$)	2.4 ± 0.1 (100 μM , $n = 30$)	1550 ± 60 (100 μM , $n = 8$)	394 ± 149 (100 μM , $n = 5$)	

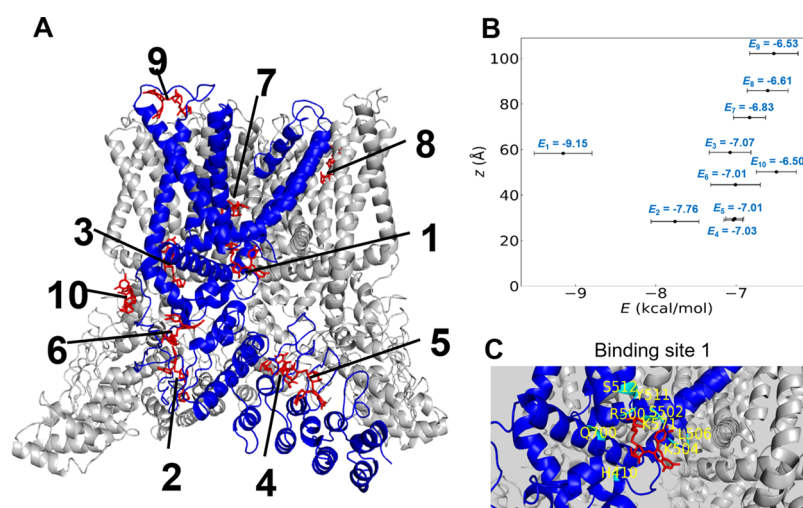


Figure 6. Binding sites of NAR to TRPV1 via molecular docking simulation. (A) Probable binding sites (10) with respect to the average binding free energy (E). The binding sites on one (highlighted in blue) of four subunits of TRPV1 are numbered from 1 to 10 in order of increasing average binding free energy. NAR is colored red. (B) Average binding free energies (E) for each binding site. Subscript i denotes the binding sites ($i = 1, \dots, 10$). The y -axis denotes the z -coordinate of the average center of mass of the top 10 lowest binding free energy binding poses of NAR. Error bars represent the standard deviations. The statistics were obtained using the top 10 binding poses (with respect to free energy values) for each site. (C) The expanded view of binding site 1 of NAR with the lowest free energy. Amino acid residues that are within 2.2 Å of any atoms in NAR at each binding site are displayed; the residues are colored cyan and the sequence is indicated in yellow.

of TRPV1 antagonists have revealed undesirable side effects. Hence, other channel modulators are being actively investigated as potential anti-inflammatory agents and analgesics, including agonists that promote TRPV1 channel desensitization in nociceptive neurons.²⁰ CAP is an example of one such pain-relieving TRPV1 agonist. It is used in various commercial analgesic creams and patches. Previously reported anti-inflammatory effects of the PN extract may also be explained through TRPV1 activation. For instance, the PN extract is known to restrain the release of the proinflammatory cytokine tumor necrosis factor- α in lipopolysaccharide-treated mice,³⁵ which is consistent with our observation that subsequent application of the PN extract considerably diminished TRPV1 current. TRPV1 channels also regulate the itching pathway of C-fiber sensory neurons, and blocking TRPV1 in sensory neurons alleviated histamine-dependent itching,³⁴ suggesting a potential role of PN extract in pruriception.

Subcutaneous inflammation begins with tissue damage or pathogen infection and the subsequent stimulation of neighboring cells to regenerate damaged tissue while simultaneously defending against infectious pathogens. Stimulated cells release various proinflammatory peptides, including calcitonin gene-related peptide and substance P, which are the endogenous activators of TRPV1. These signals mediate neurogenic inflammation such as asthma and can be ameliorated by the TRPV1 blocker CPZ.³⁶ However, genetic ablation of TRPV1 in mice enhanced inflammation in a sepsis model, while TRPV1 agonists increased anti-inflammatory signals, suggesting that a fine balance among TRPV1 signaling pathways is crucial for reducing inflammation and ensuring therapeutic efficacy. As determined by Ca^{2+} imaging experiments, 1 μM was the minimum effective concentration of NAR on TRPV1 gating, though the maximal effective concentration (100 μM) was used for the fidelity of channel current (Figures 4 and 5). Previous research has shown that 100 g of dried PN contains 64.74 mg of extractable NAR (103.7 μmol).³¹ After ingestion of PN, NAR will not be absorbed until the proximal intestine because flavonoids are predominantly absorbed in the

gastrointestinal tract, liver, and through microbial metabolism.^{37,38} Flavonoid glycosides have high bioavailability in human digestive tracts, resulting in up to 2–3% of ingested compounds absorbed into the bloodstream.³⁹ In line with this finding, daily dietary intake of 100 g of dried PN (64.74 mg of NAR) by 60 kg human can lead to the circulation of ~ 42 μmol NAR in 2.5 L of blood plasma (0.84–1.26 μM).³¹ Therefore, the concentration of NAR in the intestines and liver, where it is absorbed, is conceivably high enough to stimulate TRPV1-positive cells and visceral nerves, as it assuredly surpasses the 1 μM minimum effective concentration. As the PN extract and NAR exerted activating and desensitizing effects on TRPV1, future electrophysiological studies on dose dependence may identify the appropriate conditions for the suppression of TRPV1-mediated inflammation and chronic pain.

TRPV1 channels are also expressed in the taste buds and epithelial cells of the tongue where they contribute to taste transduction. The activity of TRPV1 channels affected salty taste signal transduction through amiloride-insensitive taste receptors in taste buds; *Trpv1* deletion increased ethanol preference in mice.^{40,41} The activation of TAS2R bitter taste receptors sensitized TRPV1 channels via a phospholipase C/protein kinase C signaling pathway.⁴² Vanillin, one of the most studied compounds in food chemistry, directly activates heterologously expressed TRPV1 channels in trigeminal ganglion neurons,⁴³ and recent evidence also suggests that vanillin stimulates TAS2R activity.⁴⁴ Future studies on the effects of NAR on TAS2Rs and TRPV1 may elucidate the mechanism underlying these unexpected effects.

Although both PN extract and NAR induced TRPV1 activation (Figures 1 and 4), the underlying mechanisms may differ because the deactivation time, which is related to channel opening time, was longer when channels were activated by the PN extract. In addition, desensitization was markedly greater when channels were activated by the PN extract (Figures 3G and 4G), suggesting that PN extract contains other constituents that modulate TRPV1 gating, including potent TRPV1 desensitizing agonists. Therefore, further purification

and screening of PN extracts may identify constituents more suitable as desensitizing agents for pain relief.

Previous studies have demonstrated that edible plants such as hot chili pepper, garlic, black pepper, and ginger activate TRPV1.^{16–18} To our knowledge, the present study is the first to report that the PN extract also acts as a potent TRPV1 agonist. In addition, several studies have reported that TRPV1 activity is attenuated by flavonoids or related glycosides such as baicalin and eriodictyol.^{45–47} Among them, myricitrin, which is abundantly isolated from *Myrica esculenta* and *Pouteria spp.*, represents the most similar glycosyloxyflavone to NAR among the known TRPV1 modulators. However, this compound also exerts an inhibitory effect on TRPV1—CAP-dependent pain was alleviated in a mouse model.⁴⁸ Therefore, our study is the first to demonstrate that NAR, as a flavonoid, activates TRPV1 channels. The present study identified a molecular mechanism that may explain the long-known effects of this ancient medicinal food. These new findings may provide important references for other physiological studies on the PN extract and TRPV1. Future studies may aim to identify additional bioactive constituents of the PN extract having potential therapeutic effects.

■ ASSOCIATED CONTENT

SI Supporting Information

The Supporting Information is available free of charge at <https://pubs.acs.org/doi/10.1021/acs.jafc.1c07724>.

Spectroscopic data of isolated narcissoside, extraction and purification procedures of NAR from the PN extract (Figure S1), isolation and determination of NAR (Figure S2), no Ca²⁺ activity in naïve HEK cells by capsaicin (CAP) and narcissoside (NAR) (Figure S3), and close-up views of the binding sites (Figure S4) (PDF)

■ AUTHOR INFORMATION

Corresponding Authors

Chun Whan Choi – Natural Product Research Team, Gyeonggi Biocenter, Gyeonggido Business and Science Accelerator, Gyeonggi-Do 16229, Republic of Korea; Phone: +82 31 8886131; Email: cwhoi@gbsa.or.kr

Gyu-Sang Hong – Brain Science Institute, Korea Institute of Science and Technology, Seoul 02792, Republic of Korea; Division of Bio-Medical Science & Technology, KIST School, University of Science and Technology, Seoul 02792, Republic of Korea; Email: gshong@kist.re.kr

Authors

Taewoong Ha – Brain Science Institute, Korea Institute of Science and Technology, Seoul 02792, Republic of Korea

Mi-Sun Kim – Brain Science Institute, Korea Institute of Science and Technology, Seoul 02792, Republic of Korea

Bokeum Kang – Brain Science Institute, Korea Institute of Science and Technology, Seoul 02792, Republic of Korea

Kyungmin Kim – Brain Science Institute, Korea Institute of Science and Technology, Seoul 02792, Republic of Korea

Seong Su Hong – Natural Product Research Team, Gyeonggi Biocenter, Gyeonggido Business and Science Accelerator, Gyeonggi-Do 16229, Republic of Korea

Taek Kang – Brain Science Institute, Korea Institute of Science and Technology, Seoul 02792, Republic of Korea;

orcid.org/0000-0001-7066-7642

Junhyuk Woo – Brain Science Institute, Korea Institute of Science and Technology, Seoul 02792, Republic of Korea
Kyungreem Han – Brain Science Institute, Korea Institute of Science and Technology, Seoul 02792, Republic of Korea
Uhtaek Oh – Brain Science Institute, Korea Institute of Science and Technology, Seoul 02792, Republic of Korea

Complete contact information is available at:

<https://pubs.acs.org/10.1021/acs.jafc.1c07724>

Author Contributions

||T.H. and M.-S.K. contributed equally to this paper; G.-S.H. and C.W.C. designed research; T.H. and M.-S.K. performed Ca²⁺ imaging and patch-clamp experiments; C.W.C. and S.S.H. performed chemical purification; J.W. and K.H. performed computational simulation; T.H., M.-S.K., B.K., K.K., J.W., K.H., T.K., and G.-S.H. analyzed data; and G.-S.H. and U.O. wrote the manuscript. All authors participated in the discussion.

Notes

The authors declare no competing financial interest.

■ ACKNOWLEDGMENTS

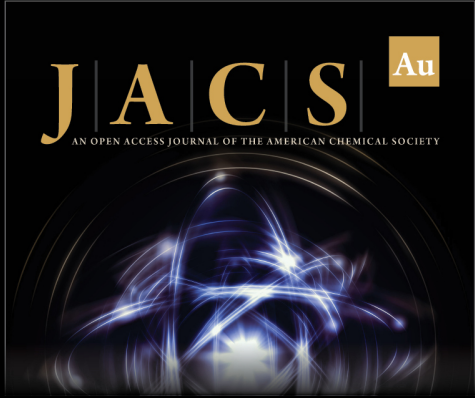
This research was supported by the National Research Foundation of Korea (NRF-2020R1C1C1010245) and an internal grant of the Korea Institute of Science and Technology (2E31502, 2E31503 and 2V09106).

■ REFERENCES


- (1) Paudel, K. R.; Panth, N. Phytochemical Profile and Biological Activity of *Nelumbo nucifera*. *Evid.-Based Complement. Altern. Med.* **2015**, *2015*, No. 789124.
- (2) Chen, S.; Li, X.; Wu, J.; Li, J.; Xiao, M.; Yang, Y.; Liu, Z.; Cheng, Y. *Plumula Nelumbinis*: A review of traditional uses, phytochemistry, pharmacology, pharmacokinetics and safety. *J. Ethnopharmacol.* **2021**, *266*, No. 113429.
- (3) Chen, G. L.; Fan, M. X.; Wu, J. L.; Li, N.; Guo, M. Q. Antioxidant and anti-inflammatory properties of flavonoids from lotus plumule. *Food Chem.* **2019**, *277*, 706–712.
- (4) Bharathi Priya, L.; Baskaran, R.; Huang, C. Y.; Vijaya Padma, V. Neferine modulates IGF-1R/Nrf2 signaling in doxorubicin treated H9c2 cardiomyoblasts. *J. Cell. Biochem.* **2018**, *119*, 1441–1452.
- (5) Zhang, X.; Wang, X.; Wu, T.; Li, B.; Liu, T.; Wang, R.; Liu, Q.; Liu, Z.; Gong, Y.; Shao, C. Isoliquinoline induces apoptosis in triple-negative human breast cancer cells through ROS generation and p38 MAPK/JNK activation. *Sci. Rep.* **2015**, *5*, No. 12579.
- (6) Tungmunnithum, D.; Pinthong, D.; Hano, C. Flavonoids from *Nelumbo nucifera* Gaertn., a Medicinal Plant: Uses in Traditional Medicine, Phytochemistry and Pharmacological Activities. *Medicines* **2018**, *5*, No. 127.
- (7) Tungmunnithum, D.; Thongboonyou, A.; Pholboon, A.; Yongsabai, A. Flavonoids and Other Phenolic Compounds from Medicinal Plants for Pharmaceutical and Medical Aspects: An Overview. *Medicines* **2018**, *5*, No. 93.
- (8) Fan, S. H.; Yang, G. G.; Zhang, J. H.; Li, J. N.; Bai, B. Q. Optimization of Ultrasound-Assisted Extraction Using Response Surface Methodology for Simultaneous Quantitation of Six Flavonoids in Flos Sophorae Immaturus and Antioxidant Activity. *Molecules* **2020**, *25*, No. 1767.
- (9) Wan, C.; Yu, Y.; Zhou, S.; Tian, S.; Cao, S. Isolation and identification of phenolic compounds from *Gynura divaricata* leaves. *Pharmacogn. Mag.* **2011**, *7*, 101–108.
- (10) Wang, J.; Gao, H.; Zhao, J.; Wang, Q.; Zhou, L.; Han, J.; Yu, Z.; Yang, F. Preparative separation of phenolic compounds from *Halimodendron halodendron* by high-speed counter-current chromatography. *Molecules* **2010**, *15*, 5998–6007.
- (11) Liu, T. T.; Cao, L. X.; Zhang, T. T.; Fu, H. Molecular docking studies, anti-Alzheimer's disease, antidiabetic, and anti-acute myeloid

- leukemia potentials of narcissoside. *Arch. Physiol. Biochem.* **2020**, DOI: 10.1080/13813455.2020.1828483.
- (12) Taslimi, P. Evaluation of in vitro inhibitory effects of some natural compounds on tyrosinase activity and molecular docking study: Antimelanogenesis potential. *J. Biochem. Mol. Toxicol.* **2020**, *34*, No. e22566.
- (13) Caterina, M. J.; Schumacher, M. A.; Tominaga, M.; Rosen, T. A.; Levine, J. D.; Julius, D. The capsaicin receptor: a heat-activated ion channel in the pain pathway. *Nature* **1997**, *389*, 816–824.
- (14) Du, Q.; Liao, Q.; Chen, C.; Yang, X.; Xie, R.; Xu, J. The Role of Transient Receptor Potential Vanilloid 1 in Common Diseases of the Digestive Tract and the Cardiovascular and Respiratory System. *Front. Physiol.* **2019**, *10*, No. 1064.
- (15) Oh, U.; Hwang, S. W.; Kim, D. Capsaicin activates a nonselective cation channel in cultured neonatal rat dorsal root ganglion neurons. *J. Neurosci.* **1996**, *16*, 1659–1667.
- (16) Dedov, V. N.; Tran, V. H.; Duke, C. C.; Connor, M.; Christie, M. J.; Mandadi, S.; Roufogalis, B. D. Gingerols: a novel class of vanilloid receptor (VR1) agonists. *Br. J. Pharmacol.* **2002**, *137*, 793–798.
- (17) Macpherson, L. J.; Geierstanger, B. H.; Viswanath, V.; Bandell, M.; Eid, S. R.; Hwang, S.; Patapoutian, A. The pungency of garlic: activation of TRPA1 and TRPV1 in response to allicin. *Curr. Biol.* **2005**, *15*, 929–934.
- (18) McNamara, F. N.; Randall, A.; Gunthorpe, M. J. Effects of piperine, the pungent component of black pepper, at the human vanilloid receptor (TRPV1). *Br. J. Pharmacol.* **2005**, *144*, 781–790.
- (19) Yekkirala, A. S.; Roberson, D. P.; Bean, B. P.; Woolf, C. J. Breaking barriers to novel analgesic drug development. *Nat. Rev. Drug Discovery* **2017**, *16*, 810.
- (20) Duarte, Y.; Caceres, J.; Sepulveda, R. V.; Arriagada, D.; Olivares, P.; Diaz-Franulic, I.; Stehberg, J.; Gonzalez-Nilo, F. Novel TRPV1 Channel Agonists With Faster and More Potent Analgesic Properties Than Capsaicin. *Front. Pharmacol.* **2020**, *11*, No. 1040.
- (21) Hong, G. S.; Lee, B.; Wee, J.; Chun, H.; Kim, H.; Jung, J.; Cha, J. Y.; Riew, T. R.; Kim, G. H.; Kim, I. B.; Oh, U. TRPV1 Confers Distinct Mechanosensitive Currents in Dorsal-Root Ganglion Neurons with Proprioceptive Function. *Neuron* **2016**, *91*, 107–118.
- (22) Jang, Y.; Lee, W. J.; Hong, G. S.; Shim, W. S. Red ginseng extract blocks histamine-dependent itch by inhibition of H1R/TRPV1 pathway in sensory neurons. *J. Ginseng Res.* **2015**, *39*, 257–264.
- (23) Trott, O.; Olson, A. J. AutoDock Vina: Improving the speed and accuracy of docking with a new scoring function, efficient optimization, and multithreading. *J. Comput. Chem.* **2010**, *31*, 455–461.
- (24) Eberhardt, J.; Santos-Martins, D.; Tillack, A. F.; Forli, S. AutoDock Vina 1.2.0: New Docking Methods, Expanded Force Field, and Python Bindings. *J. Chem. Inf. Model.* **2021**, *61*, 3891–3898.
- (25) Huey, R.; Morris, G. M.; Olson, A. J.; Goodsell, D. S. A semiempirical free energy force field with charge-based desolvation. *J. Comput. Chem.* **2007**, *28*, 1145–1152.
- (26) Weiner, S. J.; Kollman, P. A.; Case, D. A.; Singh, U. C.; Ghio, C.; Alagona, G.; Profeta, S.; Weiner, P. A new force field for molecular mechanical simulation of nucleic acids and proteins. *J. Am. Chem. Soc.* **1984**, *106*, 765–784.
- (27) Dolinsky, T. J.; Czodrowski, P.; Li, H.; Nielsen, J. E.; Jensen, J. H.; Klebe, G.; Baker, N. A. PDB2PQR: expanding and upgrading automated preparation of biomolecular structures for molecular simulations. *Nucleic Acids Res.* **2007**, *35*, W522–W525.
- (28) Olsson, M. H. M.; Søndergaard, C. R.; Rostkowski, M.; Jensen, J. H. PROPKA3: Consistent Treatment of Internal and Surface Residues in Empirical pKa Predictions. *J. Chem. Theory Comput.* **2011**, *7*, 525–537.
- (29) Head, J. D.; Zerner, M. C. A Broyden–Fletcher–Goldfarb–Shanno optimization procedure for molecular geometries. *Chem. Phys. Lett.* **1985**, *122*, 264–270.
- (30) Gürbüz, P. Flavonoid Glycosides from *Heracleum pastinaca* Fenzl. *Turk. J. Pharm. Sci.* **2019**, *16*, 191–195.
- (31) Chen, S.; Fang, L.; Xi, H.; Guan, L.; Fang, J.; Liu, Y.; Wu, B.; Li, S. Simultaneous qualitative assessment and quantitative analysis of flavonoids in various tissues of lotus (*Nelumbo nucifera*) using high performance liquid chromatography coupled with triple quadrupole mass spectrometry. *Anal. Chim. Acta* **2012**, *724*, 127–135.
- (32) Bae, C.; Anselmi, C.; Kalia, J.; Jara-Oseguera, A.; Schwieters, C. D.; Krepiak, D.; Won Lee, C.; Kim, E. H.; Kim, J. I.; Faraldo-Gomez, J. D.; Swartz, K. J. Structural insights into the mechanism of activation of the TRPV1 channel by a membrane-bound tarantula toxin. *eLife* **2016**, *5*, No. e11273.
- (33) Bujak, J. K.; Kosmala, D.; Szopa, I. M.; Majchrzak, K.; Bednarczyk, P. Inflammation, Cancer and Immunity-Implication of TRPV1 Channel. *Front. Oncol.* **2019**, *9*, No. 1087.
- (34) Shim, W. S.; Tak, M. H.; Lee, M. H.; Kim, M.; Kim, M.; Koo, J. Y.; Lee, C. H.; Kim, M.; Oh, U. TRPV1 mediates histamine-induced itching via the activation of phospholipase A2 and 12-lipoxygenase. *J. Neurosci.* **2007**, *27*, 2331–2337.
- (35) Lin, J. Y.; Wu, A. R.; Liu, C. J.; Lai, Y. S. Suppressing effects of lotus plumule (*Nelumbo nucifera* Geartn.) supplementation on LPS-induced systemic inflammation in a BALB/c mouse model. *J. Food Drug Anal.* **2006**, *14*, 273–278.
- (36) Song, J.; Kang, J.; Lin, B.; Li, J.; Zhu, Y.; Du, J.; Yang, X.; Xi, Z.; Li, R. Mediating Role of TRPV1 Ion Channels in the Co-exposure to PM2.5 and Formaldehyde of Balb/c Mice Asthma Model. *Sci. Rep.* **2017**, *7*, No. 11926.
- (37) Walle, T. Absorption and metabolism of flavonoids. *Free Radical Biol. Med.* **2004**, *36*, 829–837.
- (38) Williamson, G.; Clifford, M. N. Colonic metabolites of berry polyphenols: the missing link to biological activity? *Br. J. Nutr.* **2010**, *104*, S48–66.
- (39) Graefe, E. U.; Wittig, J.; Mueller, S.; Riethling, A. K.; Uehleke, B.; Drewelow, B.; Pforte, H.; Jacobasch, G.; Derendorf, H.; Veit, M. Pharmacokinetics and bioavailability of quercetin glycosides in humans. *J. Clin. Pharmacol.* **2001**, *41*, 492–499.
- (40) Blednov, Y. A.; Harris, R. A. Deletion of vanilloid receptor (TRPV1) in mice alters behavioral effects of ethanol. *Neuropharmacology* **2009**, *56*, 814–820.
- (41) Lyall, V.; Heck, G. L.; Vinnikova, A. K.; Ghosh, S.; Phan, T. H.; Alam, R. I.; Russell, O. F.; Malik, S. A.; Bigbee, J. W.; DeSimone, J. A. The mammalian amiloride-insensitive non-specific salt taste receptor is a vanilloid receptor-1 variant. *J. Physiol.* **2004**, *558*, 147–159.
- (42) Gu, Q. D.; Joe, D. S.; Gilbert, C. A. Activation of bitter taste receptors in pulmonary nociceptors sensitizes TRPV1 channels through the PLC and PKC signaling pathway. *Am. J. Physiol.: Lung Cell. Mol. Physiol.* **2017**, *312*, L326–L333.
- (43) Lübbert, M.; Kyereme, J.; Schobel, N.; Beltran, L.; Wetzels, C. H.; Hatt, H. Transient receptor potential channels encode volatile chemicals sensed by rat trigeminal ganglion neurons. *PLoS One* **2013**, *8*, No. e77998.
- (44) Morini, G.; Winnig, M.; Vennegeerts, T.; Borgonovo, G.; Bassoli, A. Vanillin Activates Human Bitter Taste Receptors TAS2R14, TAS2R20, and TAS2R39. *Front. Nutr.* **2021**, *8*, No. 683627.
- (45) Abbas, M. A. Modulation of TRPV1 channel function by natural products in the treatment of pain. *Chem.–Biol. Interact.* **2020**, *330*, No. 109178.
- (46) Rossato, M. F.; Trevisan, G.; Walker, C. I.; Klafke, J. Z.; de Oliveira, A. P.; Villarinho, J. G.; Zanon, R. B.; Royes, L. F.; Athayde, M. L.; Gomez, M. V.; Ferreira, J. Eriodictyol: a flavonoid antagonist of the TRPV1 receptor with antioxidant activity. *Biochem. Pharmacol.* **2011**, *81*, 544–551.
- (47) Sui, F.; Zhang, C. B.; Yang, N.; Li, L. F.; Guo, S. Y.; Huo, H. R.; Jiang, T. L. Anti-nociceptive mechanism of baicalin involved in intervention of TRPV1 in DRG neurons in vitro. *J. Ethnopharmacol.* **2010**, *129*, 361–366.
- (48) Meotti, F. C.; Luiz, A. P.; Pizzolatti, M. G.; Kassuya, C. A.; Calixto, J. B.; Santos, A. R. Analysis of the antinociceptive effect of the flavonoid myricitrin: evidence for a role of the L-arginine-nitric oxide


and protein kinase C pathways. *J. Pharmacol. Exp. Ther.* **2006**, *316*, 789–796.




JACS Au
AN OPEN ACCESS JOURNAL OF THE AMERICAN CHEMICAL SOCIETY



Editor-in-Chief
Prof. Christopher W. Jones
Georgia Institute of Technology, USA

Open for Submissions 

pubs.acs.org/jacsau  ACS Publications
Most Trusted. Most Cited. Most Read.